Modeling the momentum and heat fields in a circulation flow above an areal heat source in a stable stratified environment

A.F. Kurbatskii[1] and L.I. Kurbatskaya[2]

[1]*Institute of Theoretical and Applied Mechanics, Siberian Branch of the Russian Academy of Sciences, Novosibirsk*
[1] *Novosibirsk State University*
[2] *Institute of Computational Mathematics and Mathematical Geophysics, Siberian Branch of the Russian Academy of Sciences, Novosibirsk*

Received March 5, 2002

A computationally efficient three-equation model of the turbulent transport of momentum and heat for simulating a circulation structure over an areal heat source in a stable stratified environment is formulated and evaluated. Results of the numerical simulation demonstrate that the three-equation model is able to predict the circulation structure, which is in a good agreement with the experimental data. Effects of buoyancy on the mean temperature and vertical turbulent heat flux in the thermal stable stratified mixing layer behind a grid generating the turbulence have also been evaluated.

Introduction

Turbulence closure models are often used as tools to analyze and predict atmospheric boundary layer characteristics. In recent 20 years, numerous articles dealing with various types of flows using different models have been published.

For stratified atmospheric flows the most frequently used models are $E - \varepsilon$ models,[1] second-order closure models[2] and third-order closure models.[3,4] Together with large eddy models[5] the third-order closure models should be considered as tools for basic research because of their large computer demands.

A growing need for detailed simulations of turbulent structures of stably stratified flows motivates the development and verification of computationally more efficient closure models for applied research that should be kept as simple as possible in order to reduce the computational demands.

The ideas underlying the completely explicit algebraic models of the turbulent transport can improve the buoyant flow modeling. At present, the full second-order turbulence closure models seem to be much demanding in solving the applied modeling problems. Indeed, recent studies[6,7,8] of the stable stratified flows indicate that a model with a transport approximation including buoyancy effects might be the optimal way that combines both computational efficiency and predictive capability.

The algebraic techniques of modeling the turbulent transfer of the momentum, heat, and matter can be modified to obtain a completely explicit algebraic heat-flux model for buoyant flows. In order to avoid using the symbolic algebra software for inverting a system of algebraic equations for the turbulent heat fluxes $-\langle u_i\,\theta\rangle$ and turbulent momentum fluxes $-\langle u_i\,u_j\rangle$, it is desirable to derive an explicit algebraic heat-flux model where the heat fluxes are expressed explicitly in terms of the mean gradients and the eddy diffusivities.

Results of computational modeling and simulation of stable stratified flows[6,8] showed the importance of retaining the full prognostic equation for the variance of temperature fluctuations, allowing to correctly calculate a counter-gradient transport of heat in the upper half of the turbulent layer.

The present paper proposes and evaluates a $E - \varepsilon - \langle\theta^2\rangle$ three-parameter turbulence closure scheme that has been implemented in order to make the model more useful for stable stratified flows and air pollution applications.

In the model the eddy-exchange coefficients are evaluated from the turbulent kinetic energy (TKE) E and the viscous dissipation ε. The turbulent fluxes $-\langle u_i\,\theta\rangle$ and $-\langle u_i\,u_j\rangle$ are calculated from completely explicit algebraic models for the penetrative turbulent convection from an areal heat source (the urban heat island) with no initial momentum under calm and stable stratified environment. The performance of the three-equation model was tested by comparing the calculated results with the laboratory measurements of the low-aspect-ratio plume[9] and the LES data.[4,5] Good agreements were found.

It is well known that countergradient scalar (heat and mass) transfer takes place in a turbulent flow with strongly stable stratification. Recent investigations[10] have shown that the countergradient heat transfer is induced by large-scale motion in strongly stratified air and water flows with no velocity shear occurred.

Effects of buoyancy on the mean temperature and vertical turbulent heat flux in stable stratified grid-generated turbulence are also evaluated in this paper. We show that only the differential transfer equation for the vertical turbulent heat flux enables one to reconstruct the countergradient heat flux, i.e., the effect which is inherently nonlocal from its physical nature.

1. Turbulent circulation above an areal heat source

The penetrative turbulent convection is induced by a constant heat flux H_0 from the surface of a plate with the diameter D (Figs. 1*a* and *b*).

0235-6880/02/10 848-05 $02.00

It simulates a prototype of an urban heat island with the low-aspect-ratio plume ($z_i/D \ll 1$, z_i is the mixing height) under nearly calm conditions and stably stratified atmosphere. Fundamental fluid dynamics equations describing the circulation over the low-aspect-ratio heat island in the absence of Coriolis force and radiation are written in the axisymmetric cylindrical coordinates. Hydrostatic and Boussinesq approximations are applied to simplify the model.

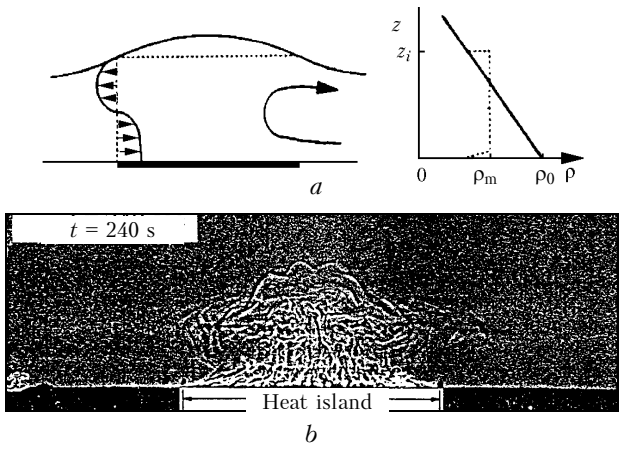

Fig. 1. Schematic diagram of the heat-island circulation including horizontal velocity distribution and vertical density profiles (z_i is mixing height, ρ_0 is density of the reference atmosphere, ρ_m is plume centerline density) (*a*). Shadowgraph picture of the heat island. At t = 240 s the full circulation is established (*b*).

In most mathematical models the thermal plume turbulence is parameterized (cf. Ref. 11). However, to analyze and understand the turbulent structure of the urban-heat-island phenomenon and the associated with it circulation, the turbulence modeling is required.

A physically correct description of the effect of stable stratification on the circulation over the heat island can be obtained by using a three-equation turbulence transport model. The TKE, its dissipation ε, and the variance of turbulent fluctuations of temperature $<\theta^2>$ are found from the differential transport equations, and the turbulent fluxes of momentum $-<u_i\, u_j>$ and heat $-<u_i\, \theta>$ are determined from completely explicit algebraic "gradient diffusion" equations. This three-equation turbulence model minimizes difficulties in describing turbulence in stable stratified flow and reduces efforts required for its numerical implementation.

1.1. Completely explicit models of turbulent fluxes

The explicit algebraic model for the turbulent heat flux vector $-<u_i\, \theta>$ can be derived from the exact transport equations[8] in the approximation of equilibrium turbulence

$$-<u_i\theta> = C_T \frac{E^2}{\varepsilon}\sqrt{2R}\frac{\partial T}{\partial x_i} - \frac{\sqrt{R}}{C_{1\theta}}\frac{E}{\varepsilon}[\{2\nu_T +$$

$$+ (1 - C_{2\theta})\, k_T\}\, S_{ij} + (1 - C_{2\theta})\, k_T\, \Omega_{ij}]\, (\partial T/\partial x_j) +$$

$$+ [(1 - C_{2\theta})/C_{1\theta}]\,(E/\varepsilon)\,\sqrt{R} g_i \beta <\theta^2>, \qquad (1)$$

where $S_{ij} = (1/2)\,(\partial U_i/\partial x_j + \partial U_j/\partial x_i)$ is the mean velocity-shear tensor, $\Omega_{ij} = (1/2)\,(\partial U_i/\partial x_j - \partial U_j/\partial x_i)$ is the mean rotational tensor, $\nu_T = C_\mu E^2/\varepsilon$ is the turbulent viscosity, $k_T = C_T\sqrt{2R}E^2/\varepsilon$ is the turbulent thermal diffusivity, $R = \tau_\theta/\tau$ is the ratio of characteristic scales of temperature (τ_θ) and dynamic (τ) turbulent fields.

Coefficients in Eq. (1) have "standard" values calibrated by modeling the homogeneous turbulence in stable stratified flows, $C_\mu = 0.09$, $C_{1\theta} = 3.28$, $C_{2\theta} = 0.4$, $C_T = 0.095$, $R = 0.6$.

Simple Boussinesq model is applied to model turbulent stresses that preserves certain anisotropy of the normal Reynolds stresses,

$$<v^2> = (2/3)\, E - 2\nu_T\, (\partial V/\partial r), \qquad (2)$$

$$<w^2> = (2/3)\, E - 2\nu_T\, (\partial W/\partial z), \qquad (3)$$

$$<u^2> = (2/3)\, E - 2\nu_T\, (V/r), \qquad (4)$$

$$-<vw> = (2/3)\, E - 2\nu_T\, (\partial V/\partial z + \partial W/\partial r). \qquad (5)$$

In equations (2)–(5) V is the mean horizontal (radial) velocity, W is the mean vertical velocity, v is the horizontal turbulent velocity fluctuation, w is the vertical turbulent velocity fluctuation, u is the azimuth turbulent velocity fluctuation, T is the mean temperature, θ is the turbulent temperature fluctuation. In Eqs. (1)–(5) and everywhere in the discussion below the capital letters and brackets <...> define mean values of variables, and lower-case letters are reserved for turbulent fluctuations.

1.2. Results of modeling

The streamlines in Fig. 2 show the main upwelling flow in the center generated by two vortices that reaches the interface layer ($z/z_i \propto 1$), and the downwelling flow in the outer region. The main specific feature is in suppression of the plume height by the stable stratification, and in the increase in the sideway flow and turbulence of the plume.

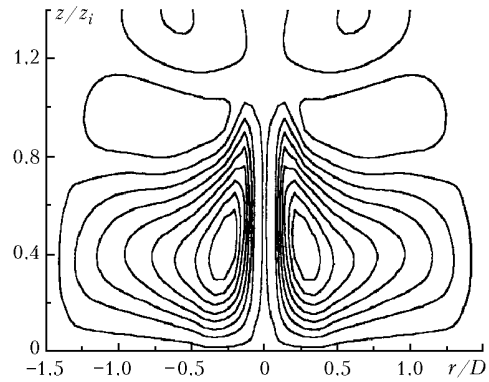

Fig. 2. Streamline contours for Fr = 0.077, Re = 8280, (Fr = $= W_D/(ND)$ is Froude number, $N = [\beta g(\partial T/\partial z)_a]^{1/2}$ is Brunt-Vaisala frequency, Re = $(W_D D)/\nu$ is Reynolds number, W_D is velocity scale).

Figures 3*a* and *b* show the radial and vertical profiles of the mean horizontal velocity. Near the surface the magnitude of the radial inflow velocity from the heat island periphery increases toward its center, reaches its maximum at the location $r/D = 0.25$, then decreases to zero at the heat island center.

The outflow velocity also increases in moving away from the center to a maximum at $r/D = 0.25$. The computed profiles of the horizontal velocity behave realistically near the surface and become zero at the surface itself unlike the measurements of Lu et al.[9] where the viscous sublayer has not been resolved.

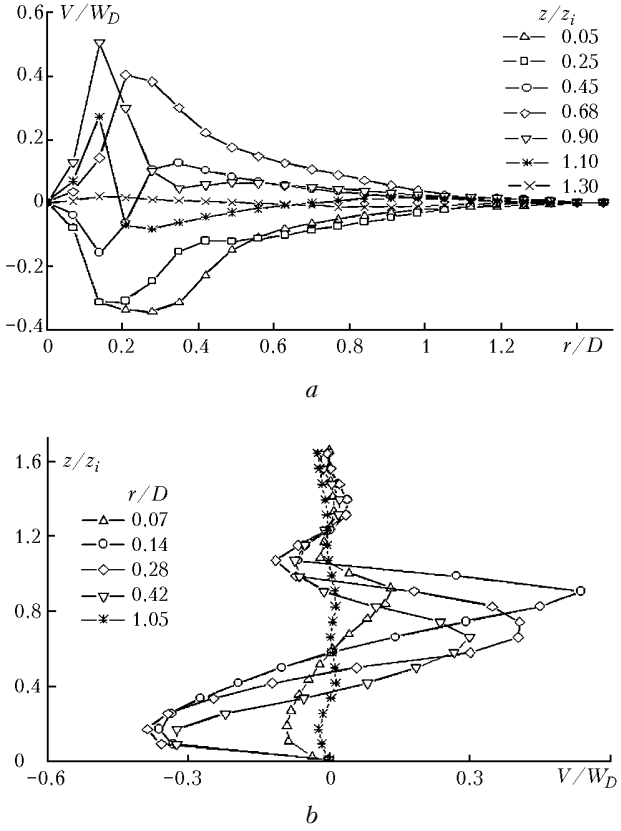

Fig. 3. Dimensionless radial velocities at different heights (*a*) and at different locations (*b*); computation for the parameters: Fr = 0.077, Re = 8280, $H_0 = 0.65$ W · cm^{-2}.

Profiles of the mean vertical velocity show that the velocity is maximum near the plume center ($r/D = 0.07$ in Fig. 4), and the maximum velocity value decreases when moving away from the center while the downwelling flow on top becomes more pronounced.

The turbulent plume structure is shown in Fig. 5 as a distribution of root-mean-square fluctuations of the vertical and horizontal turbulent velocities at the plume center.

Both experimental observations[9] and numerical simulations show that large values inside the mixing layer rapidly decrease with height above the inversion layer.

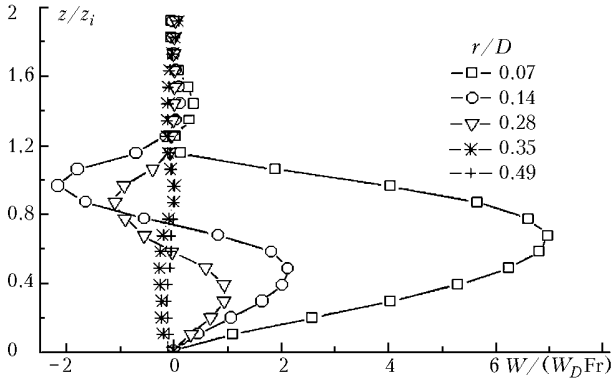

Fig. 4. Vertical velocities at different locations for the same parameters as in Fig. 3*a*.

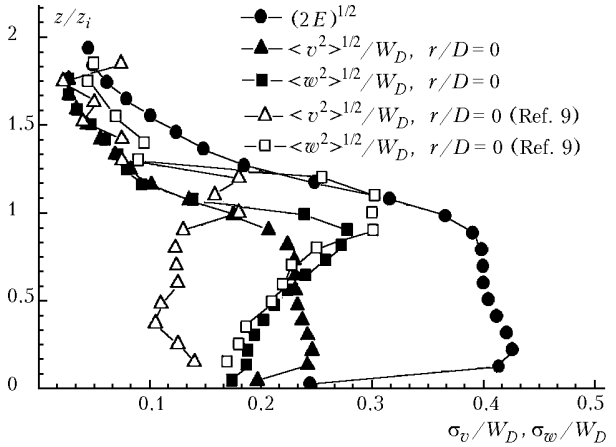

Fig. 5. Dimensionless variances of velocity on z/z_i at the center above the heat island. The laboratory data[9] (Fr = = 0.077, Re = 8280): horizontal velocity profile (△) and vertical velocity profile (□). The calculated data: horizontal velocity variance (▲), vertical velocity variance (■), and calculated intensity of turbulence, $q^2 = <u_i^2>$, (●).

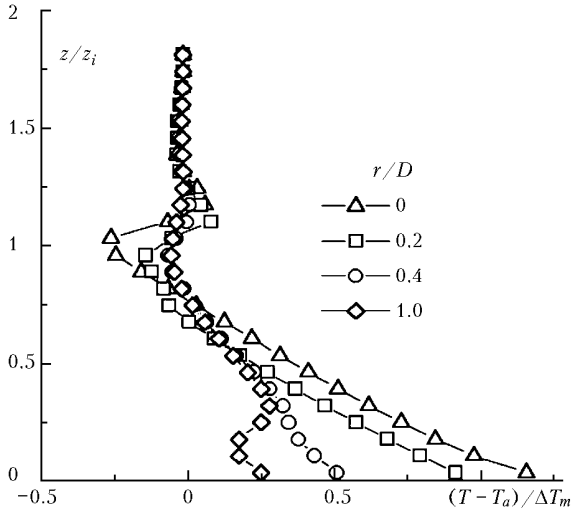

Fig. 6. Mean temperature profiles above the heat source; computations for the parameters: Fr = 0.088; Re = 4500 ($\Delta T_m = (T_m - T_a)$ is heat island intensity, T_a is ambient temperature).

It should be mentioned that the simple Boussinesq model for the Reynolds stresses not only correctly predicts characteristic features and distributions, but also satisfactorily describes their anisotropic nature. Vertical profiles of the dimensionless temperature $(T - T_a)/\Delta T_m$ (Fig. 6) show the area of strong positive buoyancy in the lower section of the plume, and the area of weak negative buoyancy near the inversion layer ($z/z_i \approx 1$).

Temperature profiles of field measurements (not shown hear) are similar to those in Fig. 6. Both experimental and field measurements reveal the universal shape of the vertical distribution of dimensionless temperature that depends neither on the Reynolds nor on the Froude number.

The dependence of the variance of turbulent fluctuations on height at the plume center is shown in Fig. 7.

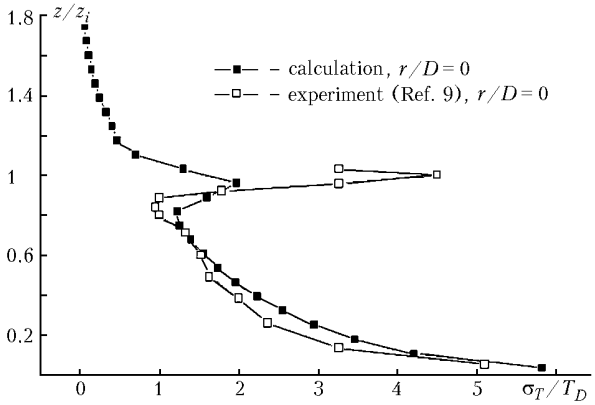

Fig. 7. Measured (□) and calculated (■) profiles of the variance of temperature fluctuations at $r/D = 0$ (Re = 4500, Fr = 0.088) ($T_D = H_0/\rho_0 c_p W_D$ is the convective scale of the temperature field).

The profile σ_T/T_D has a characteristic shape, which decreases from its maximum value at the surface to a minimum value at $z/z_i = 0.85$ as found in the experiment and predicted by the three-equation model.

2. Heat transfer in a thermally stable stratified mixing layer

Recent investigations[10] have shown that in a water tank the countergradient heat transfer is induced by large-scale motion in thermally strongly stratified flow. In this experiment hot (temperature is T_1) and cold fluids (temperature is T_2) were injected separately in the upper and lower streams upstream of the turbulence generating grid. Thus, stable thermal stratification with the initial step temperature was generated behind the gird.

Buoyancy effects on the mean temperature and vertical turbulent heat flux in this flow are modeled by the second-order closure scheme where the transport equation for the vertical turbulent heat flux as follows,

$$\frac{\partial <w\theta>}{\partial x} = -<w^2>\frac{\partial \Theta}{\partial z} - C_{1\theta}\sqrt{\frac{\varepsilon\varepsilon_\theta}{E<\theta^2>}}<w\theta> +$$

$$+\frac{\partial}{\partial z}\left(C_{S\theta}\frac{E}{\varepsilon}<w^2>\right)\frac{\partial <w\theta>}{\partial z} + (1 - C_{3\theta})\mathrm{Ri}<\theta^2>.$$

Here $\mathrm{Ri} = \beta g \Delta T M/U^2$ is the Richardson number, $\Theta = (<T> - T_2)/\Delta T$ is the mean temperature, $\Delta T = T_1 - T_2$, U is the cross section mean velocity, M is the grid size of the turbulence generating grid, β is the thermal volumetric expansion coefficient, g is the acceleration due to gravity. The model constants are identical to those used by other researchers and their values are $C_{1\theta} = 3.28$, $C_{s\theta} = 0.11$, $C_{3\theta} = 0.40$.

Numerical simulations were carried out under the same conditions as the experiments.[10] The initial profiles of the mean temperature Θ and vertical turbulent heat flux $-<w\theta>$ are taken from the experimental data measured along the cross section $x/M = 10$ behind the gird. Initial values of the TKE, dissipation ε, vertical variance of velocity $<w^2>$, temperature variance $<\theta^2>$, and dissipation of temperature fluctuations ε_θ are evaluated from the experimental data. For this reason the initial fields of all the functions sought could not be preset matched to each other.

Having in mind the damped behavior of turbulence behind the generating grid numerical results are sensitive to the initial fields of the turbulent quantities set. Figures 8*a* and *b* show that in case of weak stratification (Ri = 0.0078) the simulated results are in a good agreement with the experimental data.[10]

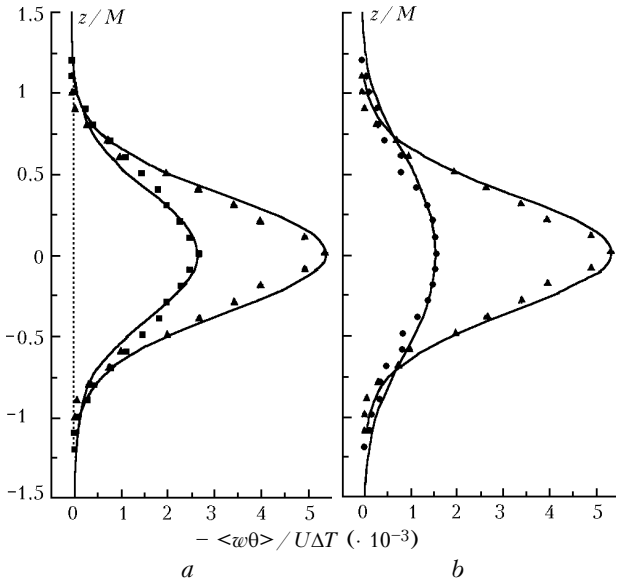

Fig. 8. Vertical profiles of the normalized vertical heat flux in the weakly stratified flow at $x/M = 10$ (▲ is experimental data,[10] solid line is calculation), $x/M = 14$ (■ is experimental data,[10] solid line is calculation) (*a*); $x/M = 14$ (● is experimental data,[10] solid line is computation) (*b*).

In the case of a strong stratification (Ri = 0.039) there is only a qualitative agreement between the numerical solution and experimental data (Fig. 9). The maximum value of computed countergradient vertical heat flux ($-<w\theta> < 0$) in the central flow region is lower than its experimental value.[10]

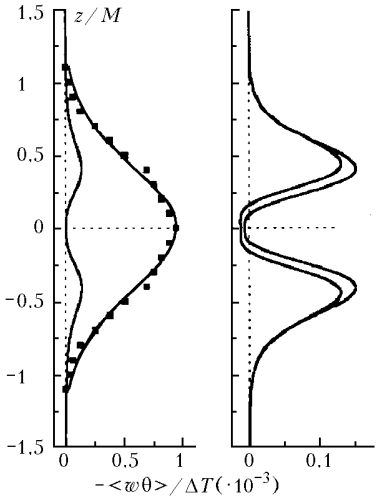

Fig. 9. Vertical profiles of the normalized vertical heat flux in the strongly stratified flow (■ is experimental data at $x/M = 10$ (Ref. 10), solid line is calculation).

It is worth noting that the use of a gradient model for the turbulent heat flux does not allow one to obtain the countergradient heat flux under conditions of strongly stable stratification. This is, most likely, caused by nonlocal nature of the turbulent diffusion that are poorly allowed for by the local models of the gradient transfer. In the case of a weak stratification the gradient models of the turbulent heat flux enable one to obtain results that agree with the experimental data.

Conclusions

The main results of this study can be summarized as follows.

The proposed model of turbulent transport reproduces structural features of the penetrative turbulent convection over the heat island. They include such subtle effects as the area of negative buoyancy that confirms the development of the dome shape (Fig. 1*b*) at the upper plume part.

The second-order closure scheme predictions of the countergradient heat transfer in the central region of stable thermally stratified flow are in qualitative agreement with the measurements.

Acknowledgments

The work was supported by the Russian Foundation for Basic Research (Grant No. 99–05–64143 and No. 01–05–85313).

References

1. P.G. Duynkerke, J. Atmos. Sci. **45**, No. 5, 865–880 (1988).
2. O. Zeman and J.L. Lumley, in: *Turbulent Shear Flows I* (Springer-Verlag, Berlin, 1979), pp. 295–306.
3. C. Andre, G. De Moor, P. Lacarrere, G. Therry, and R. du Vachat, J. Atmos. Sci. **35**, No. 10, 1861–1885 (1978).
4. V.M. Canuto, F. Minotti, C. Ronchi, and R.M. Ypma, J. Atmos. Sci. **51**, No. 12, 1605–1618 (1994).
5. F.T.M. Nieuwstadt, P.J. Mason, C.-H. Moeng, and U. Schumann, in: *Turbulent Shear Flows 8: Selected Paper from the Eighth Int. Symp. on Turbulent Shear Flows,* F. Durst et al., eds. (Springer-Verlag, Berlin, 1993), pp. 353–367.
6. A. Andren, Boundary-Layer Meteorol. **56**, No. 2, 207–221 (1991).
7. T.P. Sommer and R.M.C. So, Phys. Fluids **7**, No. 11, 2766–2777 (1995).
8. A.F. Kurbatskii, J. Appl. Meteorol. **40**, No. 10, 1748–1761 (2001).
9. J. Lu, S.P. Araya, W.H. Snyder, and R.E. Lawson, Jr., J. Appl. Meteorol. **36**, No. 10, 1377–1402 (1997).
10. K. Nagata and S. Komori, J. Fluid Mech. **430**, 361–380 (2001).
11. D.W. Byun and S.P.S. Arya, Atmos. Environ. A **24**, No. 4, 829–844 (1990).